Influence of the bubble size distribution on the bubble column flow regime

Lucas, D.; Ziegenhein, T.;

Originally published:

August 2019

International Journal of Multiphase Flow 120(2019), 103092

DOI: https://doi.org/10.1016/j.ijmultiphaseflow.2019.103092

Perma-Link to Publication Repository of HZDR:

https://www.hzdr.de/publications/Publ-28995

Influence of the bubble size distribution on the bubble column flow regime

D. Lucas[1], T. Ziegenhein[1,2]

[1]Helmholtz–Zentrum Dresden – Rossendorf, Bautzner Landstr. 400, 01328 Dresden, Germany

[2]School for Engineering of Matter, Transport and Energy, Arizona State University, Tempe, AZ 85287, USA

corresponding author: Dirk Lucas, d.lucas@hzdr.de

Abstract

The role of the bubble size dependent lateral lift force on the flow regime is experimentally investigated in a tall bubble column. In the experiments, only the initial bubble size distribution was modified by using a gas sparger with different injection needles and varying the flow through specific injection needles. The gas flow rate was kept unchanged in all experiments. Depending on the bubble size distribution homogeneous, transitional or heterogeneous flow regimes were observed. The flow regime is in good agreement with the predictions from the stability criterion obtained by a previously done linear stability analysis for poly-dispersed flow. It was found that as a rule of thumb the following criterion can be used.

If most of the gas volume is transported by bubbles smaller than the critical diameter at which the lift force changes its sign, the flow is stabilized leading to a homogeneous flow regime. If most of the gas volume is transported by bubbles larger than that diameter the flow is de-stabilized leading a heterogeneous flow regime. If the fraction of gas transported by small and large bubbles is about the same, the initial conditions remain dominant throughout the column height.

Keywords: bubble size, lift force, stability, bubble column, flow regime, regime transition

1. Introduction

The regime transition from homogenous to heterogeneous is one of the most important design parameters of bubble columns. Many theoretical and experimental investigations have been done aiming on the development of correlations to predict the transition, most of them are based on global parameters such as the gas superficial velocity (which is equivalent to the gas flow rate) or the gas volume fraction. The disadvantage of such correlations is that they are usually valid only for specific column designs and a deeper understanding of the local effect causing a regime transition is missing. The superficial velocity at which the transition occurs is usually called “transition velocity” the corresponding gas volume fraction “critical gas volume fraction” (see e.g. Krishna et al., 1991). In the present work, it is shown that all regimes can be obtained at the same superficial gas velocity at a very low gas volume fraction by just changing the initial bubble size distribution, which is in-line with a previously derived stability criterion based on the local force balance.

Experimentally the effect of system parameters has been intensively investigated during the last decades. This involves the dependency on material parameters as the gas density (Krishna et al., 1991), surface tension (Zahradnik et al., 1997, Ruzicka et al., 2008) and viscosity (Ruzicka et al., 2003). Rather complex correlations to predict the transition velocity or the critical gas volume fraction were established e.g. by Wilkinson et al. (1992), Reilly et al. (1994), Sarrafi et al. (1999) and Ribeiro (2008) depending on a combination of different material parameters like surface tension, viscosity and density of the gas and the liquid. Also the column diameter and height to diameter ratio is considered in some papers. Beside others Zahradnik et al. (1997) and Kazakis et al. (2007) investigated the influence of the sparger on the transition velocity. Ribeiro (2008) compared the existing correlations for the transition between homogeneous and heterogeneous regime with a large database on experimental data and concluded that none of these correlations was able to provide a satisfactory agreement with these data. He proposed a complex new correlation which decreased the mean deviations from the experimental data.

There are some hints regarding the influence of the bubble size distribution on the transition in some investigation, e.g. Zahradnik et al. (1997), Camaras et al., 1999, Sharaf et al. (2016). Krishna et al. (1991) observed that an increase of the gas superficial velocity above the transition velocity leads to an increasing amount of large bubbles with sphere equivalent diameter larger 5 mm, while the amount of smaller bubbles remains constant. However, it is difficult to justify whether the large bubbles trigger the transition or whether they are generated in the result of the transition. León-Becerril und Liné, (2001) concluded that non-spherical bubbles promote the transition to the heterogeneous regime. It was shown that suppression of coalescence shifts the transition velocity to larger values. Mudde et al. (2009) showed that with a specially

arranged sparger, which produces small homogeneous bubbles and minimize coalescence, the homogeneous regime can occur also for gas volume fractions much larger than the usually reported critical values. On the other hand the pure heterogeneous regime was reported by Ruzicka et al. (2001) for low gas volume flow rates.

Lucas et al. (2005) derived a stability criterion for homogeneous bubbly flow basing on force balances for the bubbles and the liquid. The linear stability analysis showed that the lift force plays a major role for the transition from homogenous to heterogeneous flows. Global effects like sparger configuration and column size only affects the criterion indirect through the change of bubble size. Interactions between local and global instabilities of a bubble column were discussed by Lucas et al. (2007).

According to Zun (1980) the lateral lift force related on the unit volume can be calculated as

$$\vec{F}_L = -C_L \rho_L \alpha \left(\vec{u}_g - \vec{u}_l\right) \times rot(\vec{u}_l), \tag{1}$$

with the subscripts g and l referring to gas and liquid respectively, ρ is the density, $\alpha$the gas volume fraction and $\vec{u}$ the velocity. As shown experimentally by Tomiyama et al. (2002) and by numerous direct numerical simulations (e.g. Dijkhuizen et al., 2010) the lift force coefficient C_L changes its sign in dependence on the bubble size. Recently the findings of Tomiyama et al. (2002) obtained for single bubbles in a linear laminar shear flow for a system with high Morton number (high viscosity) were also confirmed for low the viscid air-water system and slightly turbulent conditions (Ziegenhein et al., 2018). The well-known correlation of Tomiyama et al. (2002) fits well also for these conditions, provided the Eötvös number based on the major axis is used. With the Tomiyama correlation combined with the Wellek correlation for the bubble shape the critical sphere equivalent diameter for the change of the sign of the lift force is about 5.8 mm for the air-water system. While the Wellek-correlation is valid for contaminated water a correlation for deionized water was proposed by Ziegenhein & Lucas (2017). Using this correlation the critical diameter for the change of the sign is about 5.28 mm.

For a positive lift force coefficient C_L, which is valid for bubbles smaller than the critical diameter, bubbles rising in a liquid shear flow migrate towards lower liquid velocity while large bubbles ($C_L < 0$) migrate toward regions with higher liquid velocity, see Figure 1.

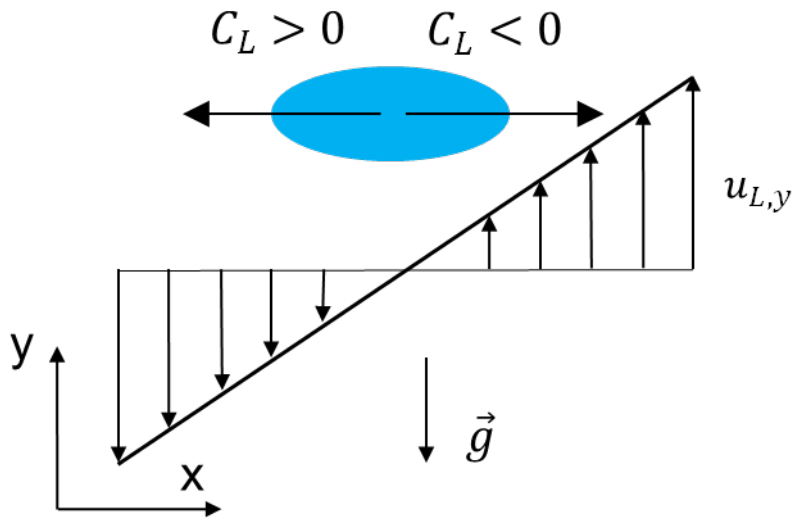

Figure 1 Direction of the lateral lift force in a liquid shear field with $u_{L,y}$ the liquid velocity in the direction of gravity $\vec{g}$ and C_L the lift force coefficient.

In a mono-disperse homogeneous bubbly flow no gradient of the liquid velocity occurs, i.e. the lift force vanishes. In case of a disturbance of the flow, e.g. if some more bubbles collect at a position in space, the resulting locally larger gas volume fraction leads to a local acceleration of the liquid, see Figure 2. Because of this acceleration gradients of the liquid velocity field are generated and cause a lift force. For small bubbles with a positive sign of the lift force coefficient the lift force acts to move the bubbles away from the position of the disturbance and thus stabilizes the flow. For large bubbles with a negative lift force coefficient the effect is vice versa. More and more large bubbles are attracted toward the position of the disturbance what destabilizes the flow.

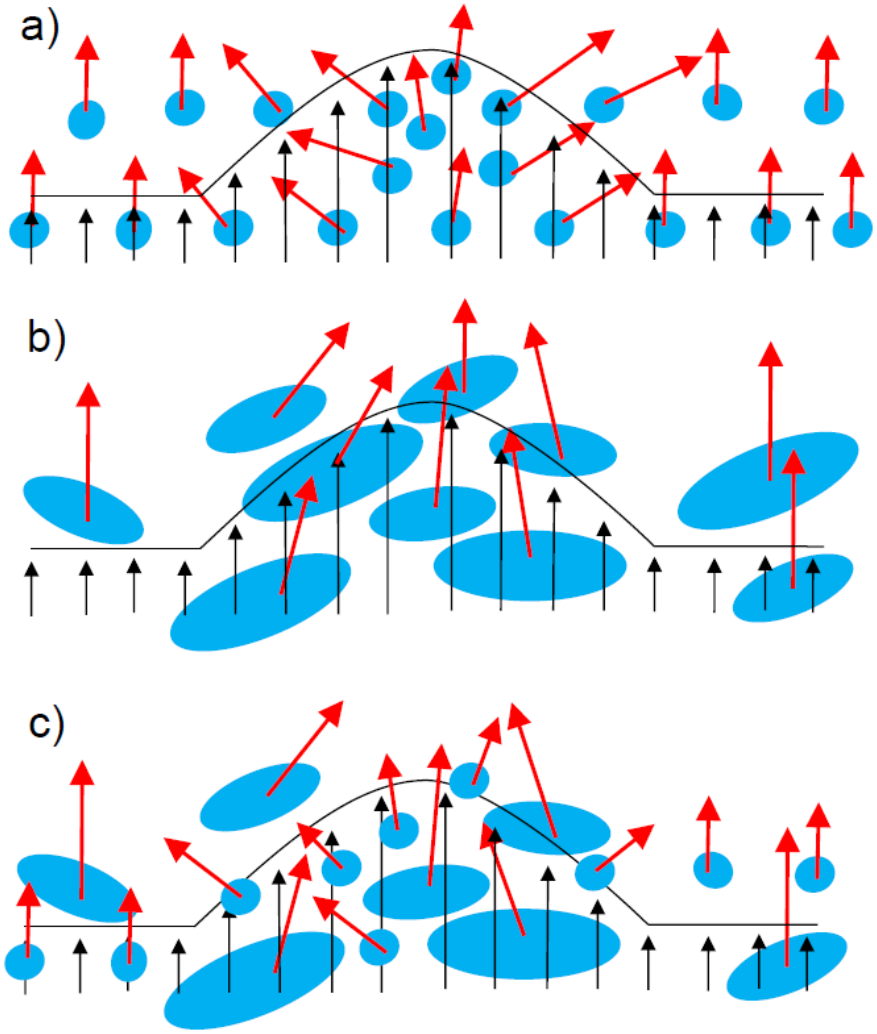

Figure 2 Disturbance of a homogeneous bubbly flow: a) mono-disperse small bubbles move away from the disturbance canceling it out, b) mono-disperse large bubbles are attracted by the distortion further increasing it, c) in poly-disperse flow separation of small and large bubbles occur

Considering the feedback of such small disturbances on themselves a linear stability analysis was done by Lucas et al. (2005). In the result a stability criterion was obtained for bimodal bubbly flows with one group of small and one group of large bubbles. In a next step it was extended for N bubble size groups (eq. (2)) and for a continuous bubble size distribution (eq. (3)). Here d_b is the sphere equivalent bubble diameter and C_D the drag force coefficient. The expression on the left-hand side of eq. (2) is called stability parameter in the following.

$$\sum_{i}^{N} \frac{\alpha_i C_{L,i} d_{B,i}}{C_{D,i}} > 0 \tag{2}$$

$$\int_{0}^{\infty} \frac{C_L(d_b) \frac{\mathrm{d}\alpha}{\mathrm{d}d_b} d_B}{C_D(d_b)} \mathrm{d}d_B > 0 \tag{3}$$

The criteria were found to fit well with the experimental results of Xu et al. (2005) and Harteveld (2005). The lift-induced flow instability was also shown in agreement with experimental findings of Akbar et al. (2013). Also homogeneous regime at very high gas volume fraction observed by Mudde et al. (2005) and the pure heterogeneous regime reported by Ruzicka et al. (2001) can be explained by these stability criteria. However, a clear experimental proof of the criteria is still missing. For this reason dedicated experiments were conducted in a high aspect ratio bubble column for air/purified water to investigate the development of the flow regime over the height for different inlet bubble size distributions.

A specific sparger allows modifying the bubble size distribution at the inlet. Due to this variation, the stability criterion was manipulated from ‘strong’ negative to ‘strong’ positive. The total gas volume flow was fixed to 1.0 l/min for all experiments. The change of only the bubble size distribution led to completely different flow structures at the same superficial gas velocity and confirmed the stability criterion experimentally.

2. Experiments

2.1 Experimental setup and test matrix

To investigate the flow structure in a bubble column depending on the bubble size distribution a rectangular bubble column with a width of 112.5 mm, a depth of 50 mm and a height of 2000 mm was used, see Figure 3a. It was filled with deionized water up to a height of 1800 mm. Air was injected via 6 needles at the bottom of the column. The air volume flow rate was fixed to 1.0 l/min for all experiments. Needles with an inner diameter of 0.12 mm, 0.3 mm, 0.6 mm, 0.9 mm, 4.0 mm and 6.0 mm were used to vary the bubble size distribution. They were arranged in two sparger groups. Group 1 consists of 4 equal needles, group 2 of two equal needles. The configuration of the groups and the combinations of needles used is presented in Figure 3. Beside by the

use of different needles also the bubble size distribution was also varied by different relative flow rates through both sparger groups keeping the total volume flow rate always at 1 l/min. In the test matrix presented in Figure 3c the columns stand for different relative flow rates (90%, 70%, 60%, 55%, 40%, 25% and 10% air flow through group 1) and the lines for different combinations of needle sizes. The identifier for each single experiment consists of two parts, the first one stand for the needle size (S – small, N – normal, 09 – 0.9 mm, 4 – 4.0 mm, 6 – 6.0 mm), the second for the fraction of the flow rate (in %) supplied through sparger group 1. Due to these variations, the stability criterion was manipulated from ‘strong’ negative to ‘strong’ positive.

The arrangement of the needles as well as the vertical alignment of the column was done very carefully to avoid all disturbances, which may influence the flow structure. The experiments were done using de-ionized water, which was renewed every experiment.

Measurements were done in 4 height positions: 50 mm, 600 mm, 1200 mm and 1600 mm above the column bottom.

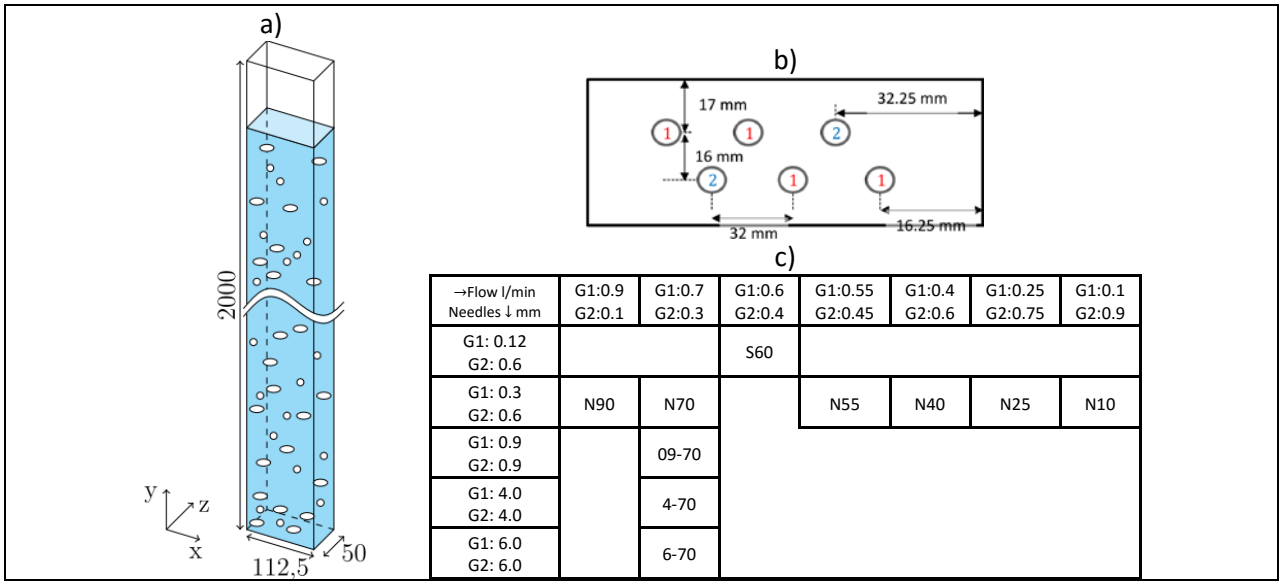

→Flow l/min Needles ↓ mm	G1:0.9 G2:0.1	G1:0.7 G2:0.3	G1:0.6 G2:0.4	G1:0.55 G2:0.45	G1:0.4 G2:0.6	G1:0.25 G2:0.75	G1:0.1 G2:0.9
G1: 0.12 G2: 0.6			S60				
G1: 0.3 G2: 0.6	N90	N70		N55	N40	N25	N10
G1: 0.9 G2: 0.9		09-70					
G1: 4.0 G2: 4.0		4-70					
G1: 6.0 G2: 6.0		6-70					

Figure 3 Experimental setup: a) Sketch of the column, b) sparger arrangement, c) test matrix

2.2 Measuring methods

To calculate the stability criterion, the gas volume fraction and bubble sizes need to be measured. In addition, the liquid velocity field is important to characterize the flow.

Since the amount of bubbles of different sizes has to be determined, the gas volume fraction and bubble size have to be measured simultaneously. This is realized by identifying the bubbles from pictures taken over time from the bubbly flow (see Figure 4).

In the following, the method to identify the bubbles is explained and the liquid velocity measurements are briefly introduced, detailed information can be found in Hessenkemper & Ziegenhein, 2018.

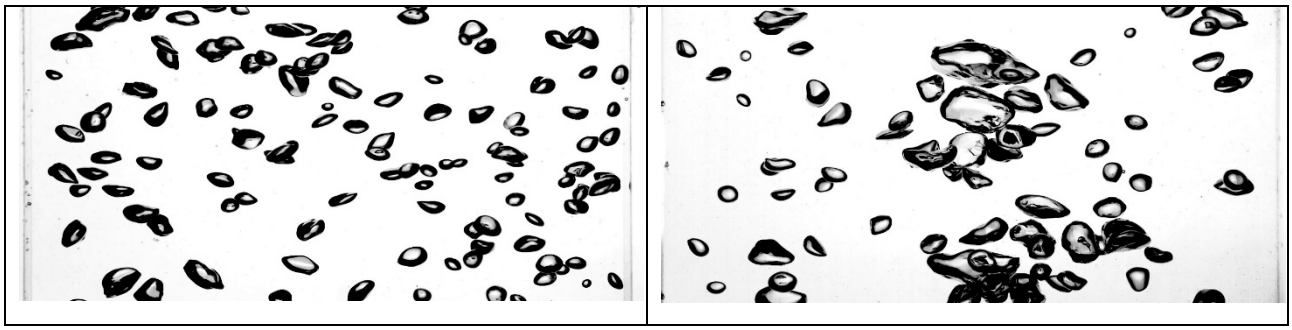

Figure 4 Pictures of the bubbly flow that are used to determine the gas volume fraction profiles and bubble sizes. Left for S60 and right for N40, 1600 mm above the sparger

The pictures of the flow were taken with an AOS Q-VIT high-speed camera and a 135 mm f2.0 Walimex Pro lens. The setup was calibrated so that the entire width and depth of the bubble column is recorded. Due to the long distance between the camera and bubble column (over 3 m) and the thin geometry (0.05 m), perspective errors can be neglected. In order to identify overlaid bubbles, a burst of ten pictures with 250 fps was recorded. This procedure is in detail explained in Ziegenhein, et al., 2016.

The bubbles are identified semi-automated from the raw pictures (Figure 5a). With a Canny Edge Detector (Canny, 1986), the edges of the bubbles (Figure 5b) are identified (Figure 5c). Afterwards, the edges are segmented by hand with a Graphical User Interface based on our own software package. Finally, ellipsoids are fitted to the bubble outline (Figure 5d).

a)

b)

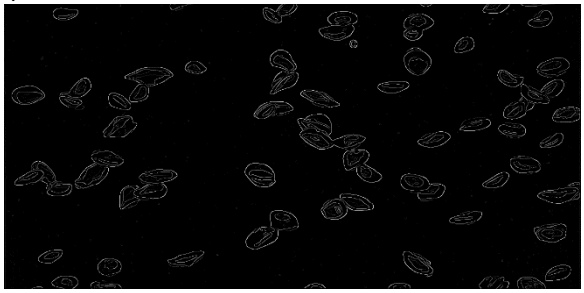

c)

d)

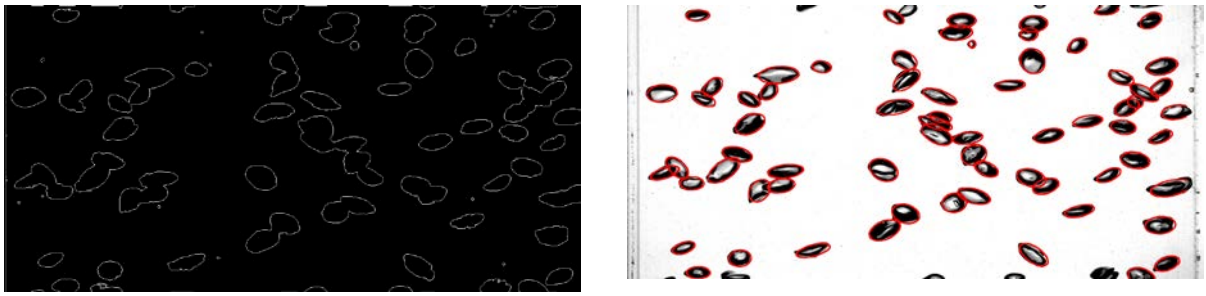

Figure 5 Identifying bubbles from the recorded pictures.

For every measuring height, at least 4000 bubbles were picked. Pictures were randomly selected from a 30 minutes measuring time. The bubble size is defined in the present work as the spherical equivalent diameter of the volume equal to the solid of revolution of the fitted ellipsoid. The major axis is defined as the longest possible chord of the projected bubble and the minor axis the longest chord perpendicular to the major axis.

Since all bubbles, including the overlaid bubbles, are identified with the present method, a gas fraction profile can be calculated. The bubble column is divided into ten virtual volume cells, which extend over the complete column depth since the position of the bubbles in depth direction is unknown. With the bubble position and the positon of the fitted ellipses, the intersection of every bubble with the volume cells is calculated. Now, the gas content in every virtual volume cell is known and the gas fraction profile can be easily calculated. Detailed information about this method and an error estimation can be found in Ziegenhein & Lucas, 2019.

In order to use Eq. (2), the identified bubbles were divided in bubble size classes, which are identified with the subscript i, of 0.25 mm width. The partial gas volume fraction, α_i, was calculated based on the bubble volume in the bubble size class. The bubble diameter of each class $d_{B,i}$ is the Sauter diameter of the bubbles in the bubble size class. Based on $d_{B,i}$, the drag and lift coefficients $C_{D,i}$ and $C_{L,i}$ are calculated according to Tomiyama 1998 and Ziegenhein et al. 2018, respectively:

$$
\begin{aligned}
C_{D,Stokes} &= \frac{48}{Re_B} \\
C_{D,Meso} &= \frac{16}{Re_B}(1.0 + 0.15 Re_B^{0.687} \\
C_{D,Wobbling} &= \frac{8}{3}\frac{Eo}{(Eo+4)} \\
C_D &= \max\left(\min\left(C_{D,Stokes}, C_{D,Meso}\right), C_{D,Wobbling}\right)
\end{aligned}
\tag{4}
$$

$$
\begin{aligned}
C_L &= 0.002 Eo_\perp^2 - 0.1 Eo_\perp + 0.5 \quad , \quad Eo_\perp < 10.5 \\
C_L &= -0.33 \quad , \quad Eo_\perp > 10.5
\end{aligned}
\tag{5}
$$

Here, Eo is the Eötvös number

$$Eo = \frac{g(\rho_l - \rho_g)d_b^2}{\sigma} \tag{6}$$

and $Eo_\perp$ the modified Eötvös number calculated according to eq. (6) but with the major axis of the bubble instead of the sphere equivalent diameter according to Ziegenhein et al. (2017):

$$d_\perp = d_B \sqrt[3]{1 + 0.65Eo^{0.35}}\,, \tag{7}$$

Using these data the stability parameter according to eq. (2) can be calculated.

A Particle Tracking Velocimetry (PTV) method with a backlighting, which is described in a previous publication (Hessenkemper & Ziegenhein, 2018), was used to measure the liquid velocity. Since a contamination of the flow needs to be prevented, a very low tracer concentration was used (Figure 6). The particle identification is based on an own developed Hough transformation (Hessenkemper & Ziegenhein, 2018). The depth of field was calibrated with test particles glued between 1mm thick glass plates to 4 mm. The Hough transformation is calculated with one-quarter sub-pixel accuracy. The particle shadows are fitted afterwards to a two-dimensional Gaussian function so that a higher sub-pixel accuracy was reached. After 30 minutes of measuring time, enough particles were tracked to obtain a smooth velocity profile. A hold processor was used in order to treat the bias sampling in multiphase flows (Ziegenhein & Lucas, 2016).

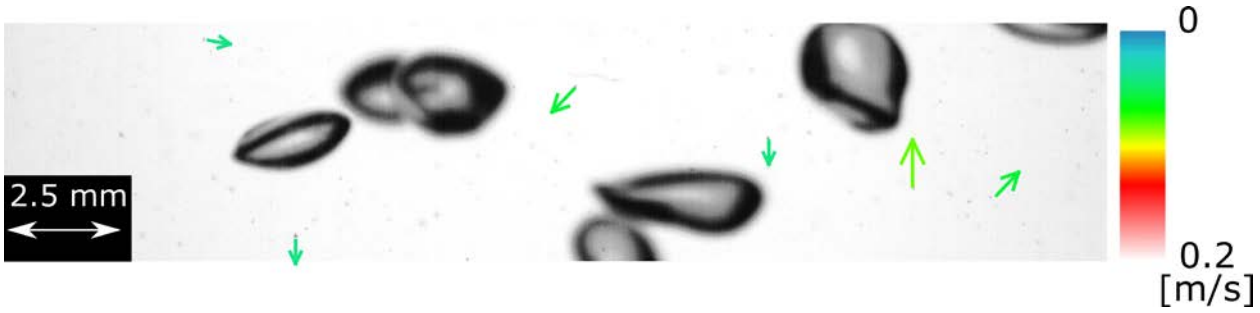

Figure 6 Velocity vectors from tracked tracer particles for N25 at 1600 mm

2.4 Criteria to identify the flow regime

The homogeneous and heterogeneous flow regimes clearly differ in the local bubble distribution over the column width. While the bubbles are equally distributed in case of homogeneous flows a clear concentration of bubbles at a position is visible in the corresponding snapshots. From the videos a plume-like behavior can be observed for

the heterogeneous regime. For a more objective distinction between the homogeneous and heterogeneous flow regimes, the gas volume fraction and liquid velocity profiles along the column width can be used. In a homogeneous flow, both profiles are rather flat, while they show a clear core peak in the heterogeneous regime, which is connected with strong circulating flow in the column, see Figure 7.

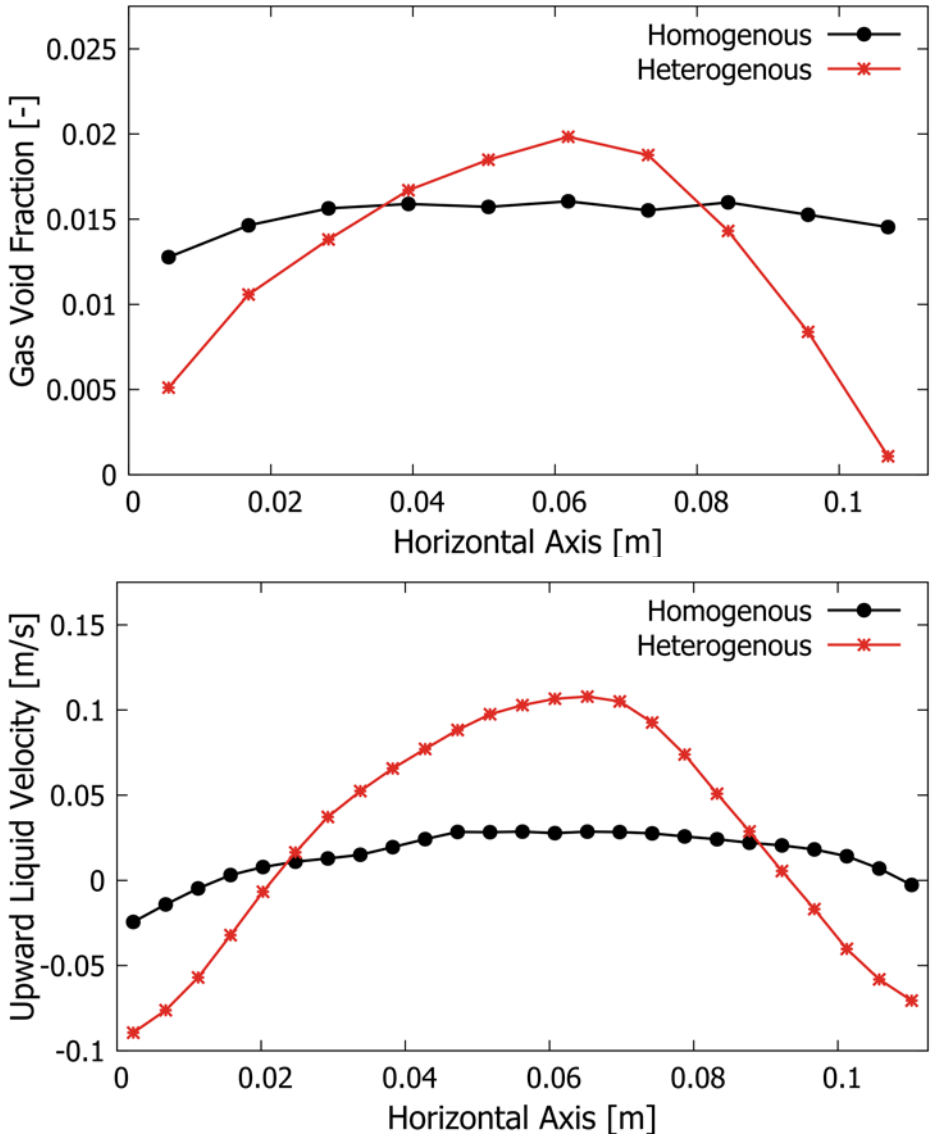

Figure 7 Typical gas volume fraction and liquid velocity profiles for the homogeneous and the heterogeneous flow regime (Homogeneous: N90, 1600 mm, Heterogeneous: 6-70, 1600 mm)

3. Results

The stability parameter according to eq. (2) for all 10 experiments is shown for height positions 50, 600, 120 and 1600 mm in Figure 8. The gas flow rate of 1 l/min led to a low gas volume fraction with maximum local values of 2 %. Because of this low gas volume fraction coalescence plays a minor role and the change of the parameter along the column height is moderate. For the green and red marked lines a clear assignment to homogeneous and heterogeneous regime can be done, respectively, according to the criteria presented in Section 2.4. For the cases given with black lines the profiles don't show clear trends to form a core peak or a flat profile. For this reason, they are marked as transition cases. Such transition cases occur since the bubbles need time to form a regime. In addition, bubble coalescence and breakup may have an influence. Therefore, if the column would be taller, these transitions would likely form a heterogeneous or homogenous regime. According to the stability analysis, the bubbly flow should be stable in case of a positive parameter and instable for a negative one. It can be expected that the effect is stronger as larger the absolute value of the stability parameters are in the positive as well as in the negative region. For this reason, the two extreme cases for the most negative parameter 6-70 and N-90 are discussed first.

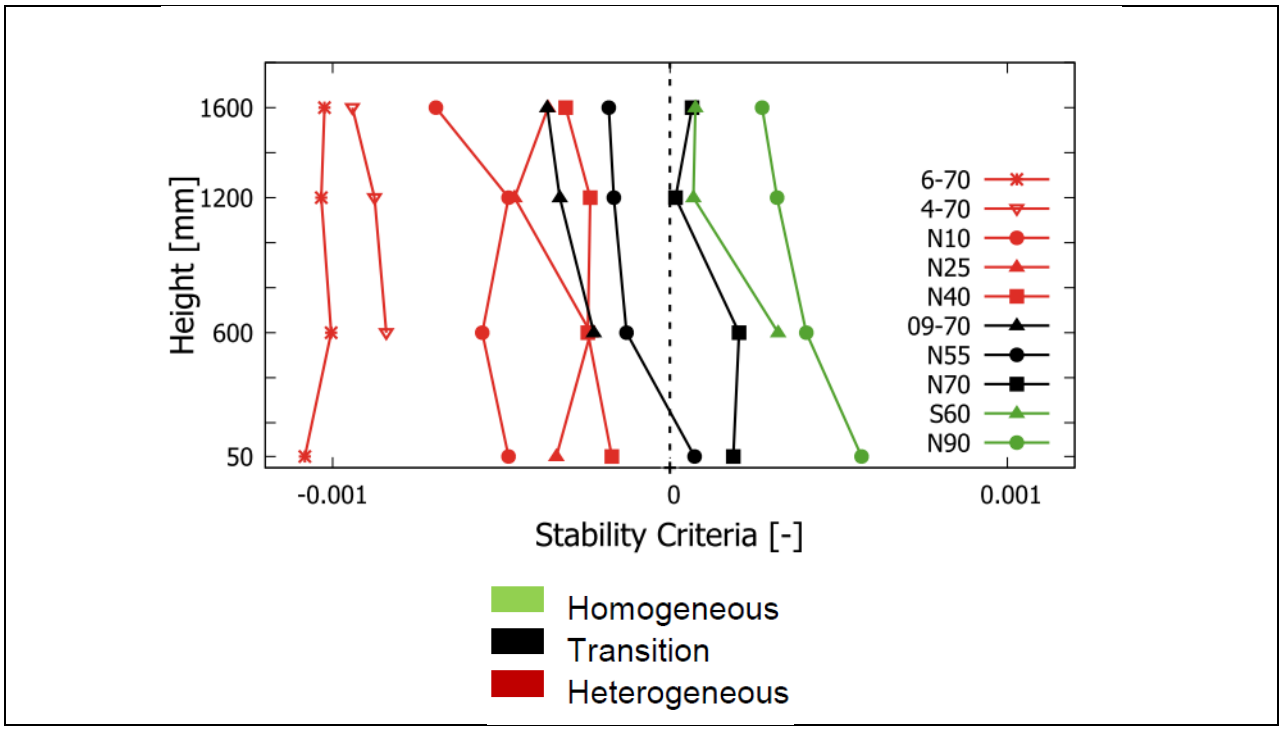

Figure 8 Stability parameter according to eq. (2).

Figure 9 shows some snapshots, bubble size distributions, gas volume fraction and liquid velocity profiles for case 6-70. As it can be seen from the bubble size distribution, Figure 9a, almost all bubbles are larger than the critical bubble size at which the lift force changes its sign (5.23 mm sphere equivalent diameter). For all height positions, the gas

volume fraction (Figure 9c) and liquid velocity profiles (Figure 9d) are center-peaked. At the lower distances still the influence of the injector with a double peaked profile is visible, but there is a clear trend to form strong center peaks which characterized the heterogeneous flow regime. This is also reflected qualitatively in the snapshots shown in Figure 9d.

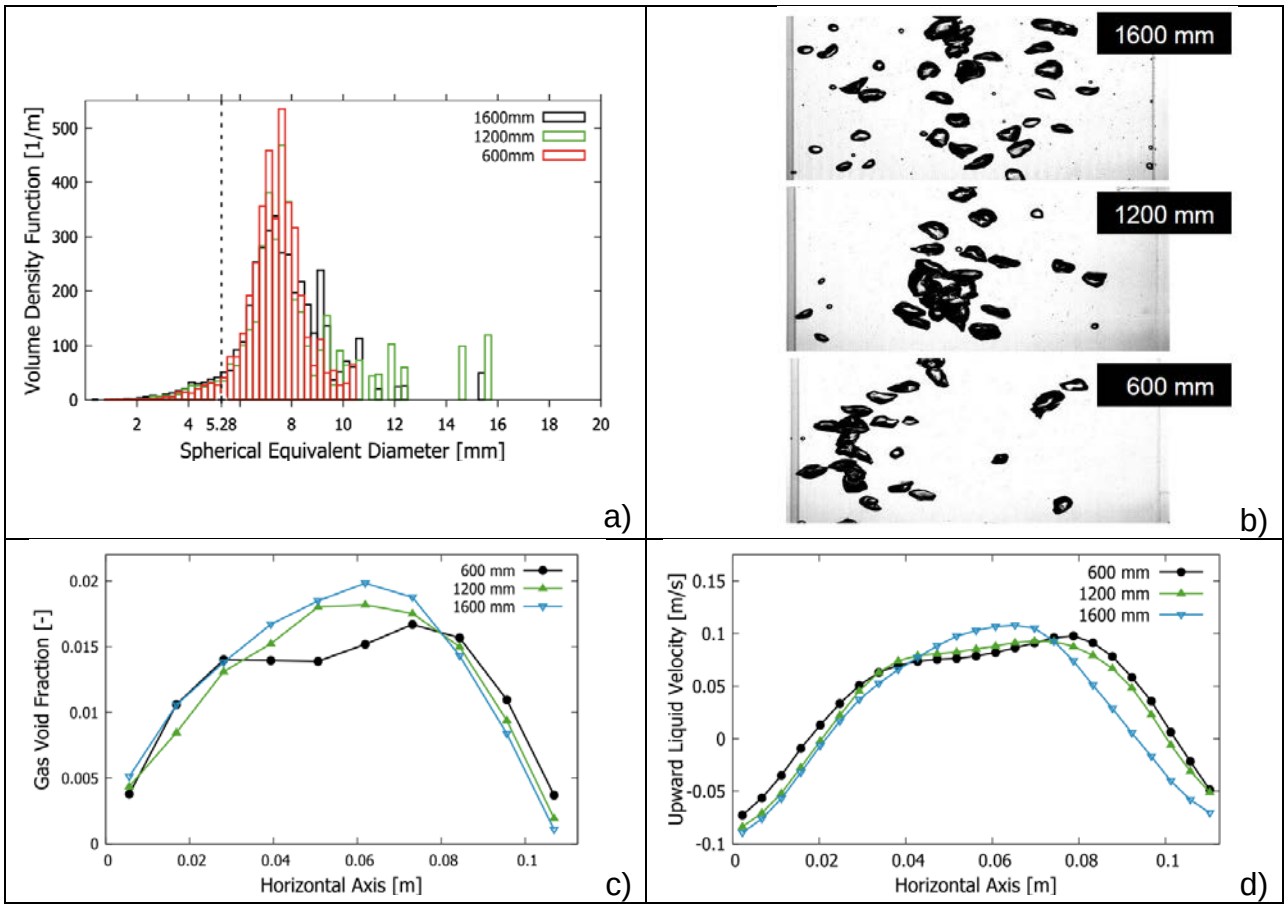

Figure 9 Results for case 6-70 (pure heterogeneous): a) bubble size distribution, b) snapshots of the flow, c) gas volume fraction profile, d) liquid velocity profile

For the case with the largest stability parameter, the corresponding results are depicted in Figure 10. Now the larger amount of the gas is transported by bubbles smaller than the critical diameter (see Figure 10a). The bubbles are homogeneously distributed in the columns for all heights (see Figure 10b). Accordingly, the gas volume fraction (Figure 10c) and liquid velocity (Figure 10d) profiles are flat, i.e. the typical characteristics of a homogeneous bubble column can be found. It should be pointed out that the only difference between the experiments 6-70 and N90 is the size distribution of the bubbles – the gas flow rate is exactly the same! It should also be emphasized that the gradients along the height are intensified for the inhomogeneous regime and flattened out for the homogenous regime, which is the leading effect described by the stability analysis.

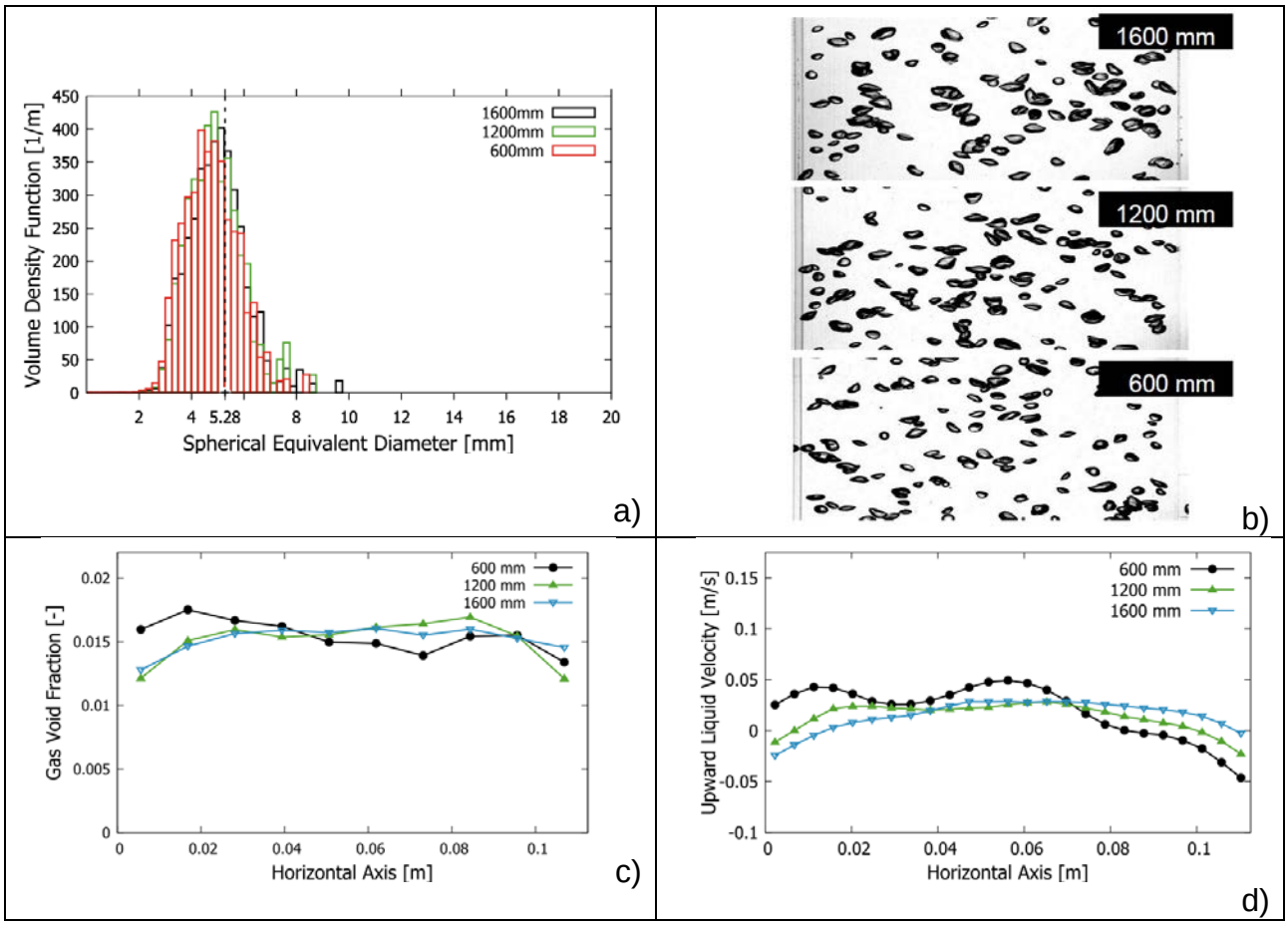

Figure 10 Results for case N90 (pure homogeneous): a) bubble size distribution, b) snapshots of the flow, c) gas volume fraction profile, d) liquid velocity profile.

For the points N70 and N55, which have the same volume flow ratio of the spargers as the pure homogeneous point N90 but larger bubbles, the gradients and profiles do not change over the height, which is why they are considered as transition points. In both cases, double peaked profiles of the liquid velocity are observed for all height positions (Figure 11). It is more pronounced in case N55 than in case N70. For case N55 (and also in case 09-70, not shown here) the double peaked profile also holds for the gas volume fraction while a slightly asymmetric profile is observed for 1200 mm and a rather flat profile for 1600 mm. There is no clear effect visible that the flow tends to stabilize or destabilize along the column. The constant profiles over the column height and that the gradients are not amplified or flattened out is in agreement with the stability analysis, which provides very small stability criteria. The volume fraction carried by bubbles smaller and larger than the critical diameter at which the lift force changes its sign is almost equal for both cases.

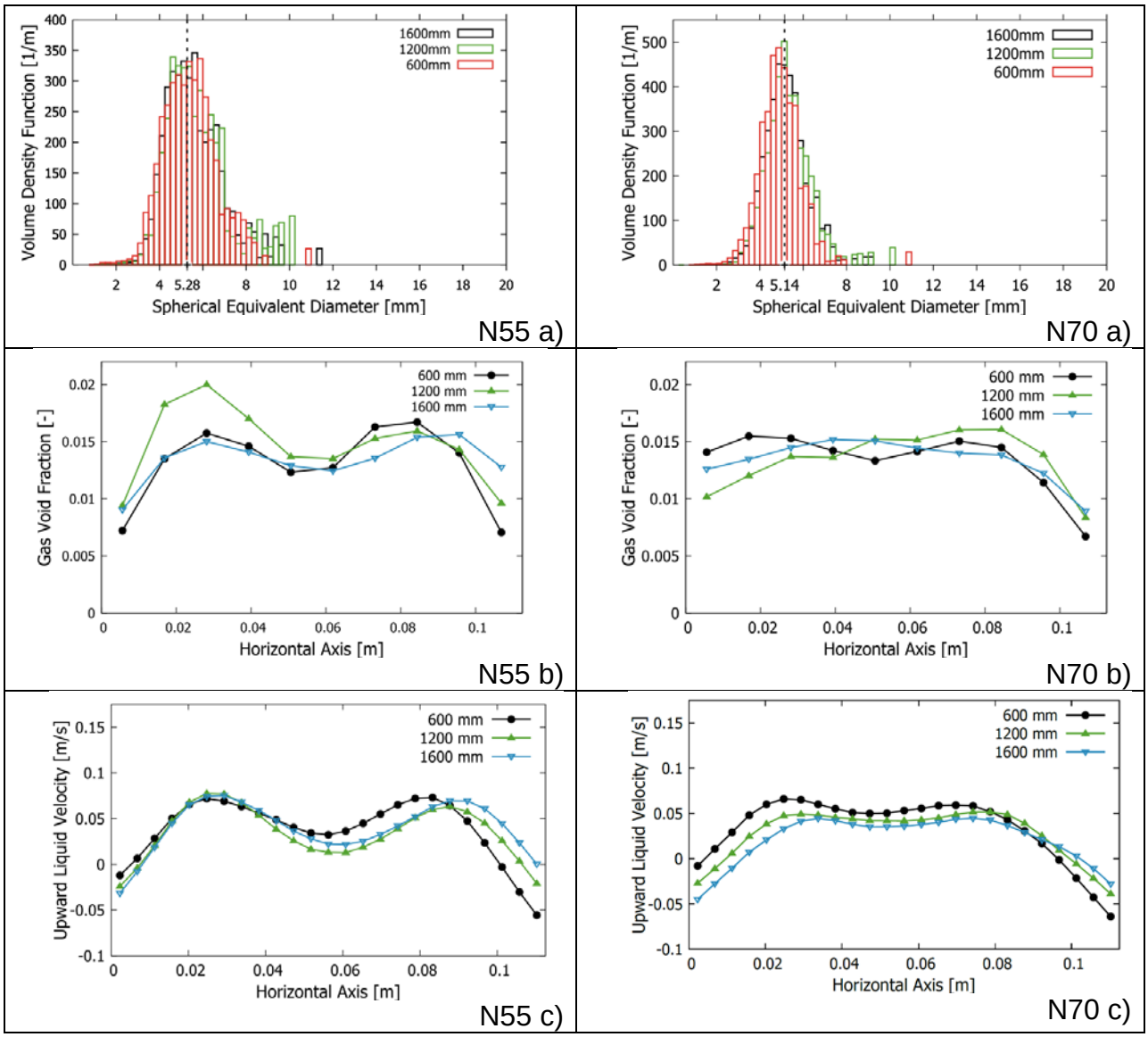

Figure 11 Results for the transition cases N55 (left) and N70 (right): a) bubble size distribution, b) gas volume fraction profile, c) liquid velocity profile.

The double peak structure caused by the injection can also be found for the lower measuring planes in the neighboring cases N40 in region of negative stability parameters and S60 in the region of positive stability parameters (see Figure 12). For higher measuring planes a clear transition to a core peak, i.e. a transition to heterogeneous flow is found for case N04 with the negative stability parameter. For case S60 the trend is not that clear. While the initial asymmetry of the velocity profile is smoothed out also some tendency to form a core peak is visible gas in the volume fraction profile. As shown in Figure 8 the stability parameter becomes smaller for this case with increasing height. This is caused by coalescence which also can be seen in the bubble size distributions, see Figure 12 S60 a). This shifts the fraction of gas volume

fraction transported by small bubble close to the value for large bubbles. However, the snapshots and the liquid velocity profiles show that the flow is still more or less homogeneous in this case. For this reason the case is still classified as homogeneous. In contrast in case N40 the larger part of the gas is transported by large bubbles.

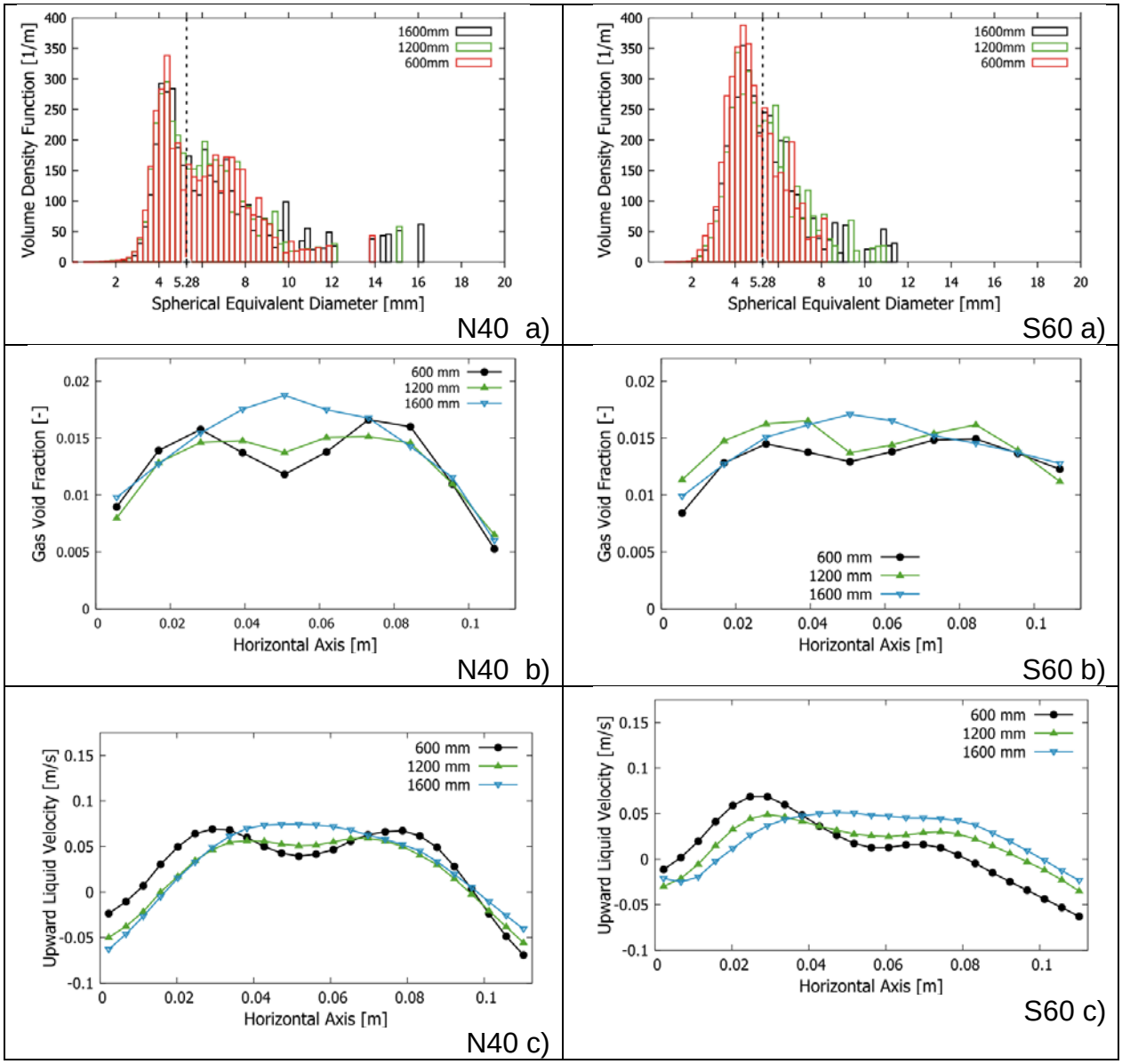

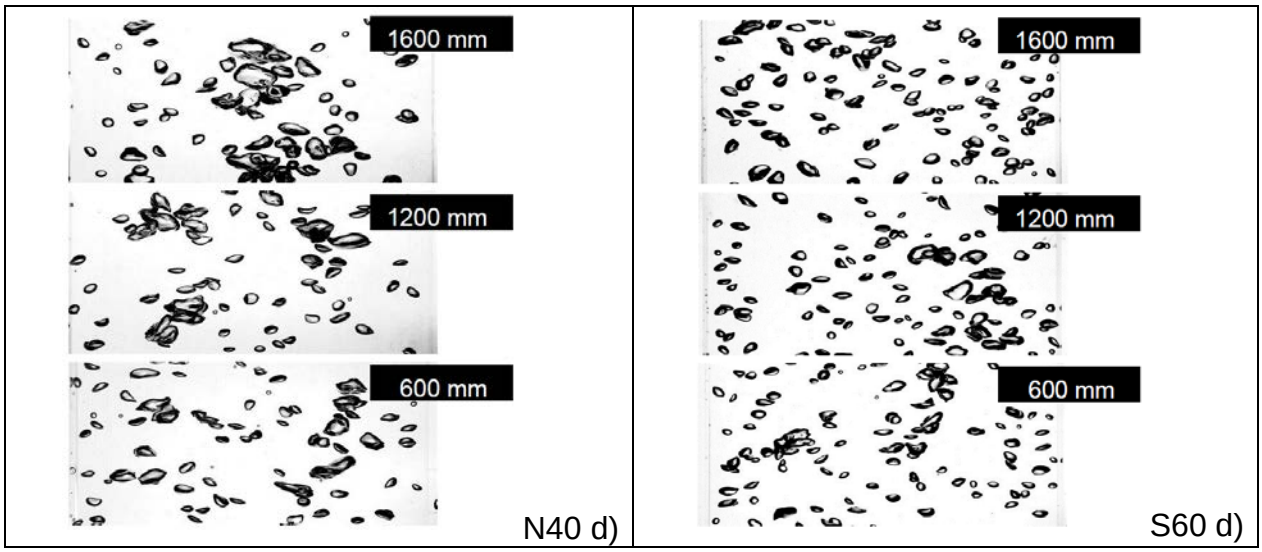

Figure 12 Results for inhomogeneous case N40 (left) and homogenous case S60 (right): a) bubble size distribution, b) gas volume fraction profile, c) liquid velocity profile, d) snapshots of the flow

Case N40, N55 and S60 start all with a double peak structure at the bottom; but they are classified as inhomogeneous, transition, and homogeneous, respectively. To investigate this behavior in more detail, the development of the gas void fraction profiles for the bubbles smaller and larger than the critical diameter over the column height are shown in Figure 13. For case N40, the profile for the large bubbles develops from a double peak to a center peak and the profile for the small bubbles develops vice versa from a center peak to a wall-peak. This behavior is why it is classified as inhomogeneous, since the center peak of the large bubbles determines the flow field and the liquid velocity shows a center peak (see Figure 12c left). As discussed above, the profiles are stable for N55: the large bubbles stay in their double peaks and the small bubbles show a center peak. For S60, the same behavior can be observed as for N40, the large bubbles migrate to the center and the small bubbles migrate to the walls. However, enough small bubbles exist to counteract the large bubbles in the center so that a more or less flat velocity profile is observed (see Figure 12c right). Therefore, S60 is considered as stabilizing and not transition. This behavior of the small bubbles to counteract the large bubbles can be observed for all cases shown in Figure 13; the small bubbles always accumulate where the large bubbles have a minimum. This observation is exactly the statement of the linear stability analysis performed by Lucas et al. (2005): The small bubbles tend to homogenize the flow.

Whether the bubbly flow creates a center peak or a double peak for the large bubbles, is not given by the local stability criteria. This might be determined by the global scales, which underlines the importance to consider global and local scales when defining stable and instable flow regimes. In addition, coalescence plays an important role for the

present stability criteria, since coalescence events can shift the stability criteria from positive to negative values, as observed for S60 (see the shift in the profile for the large bubbles from 600mm to 1200mm in Figure 13f).

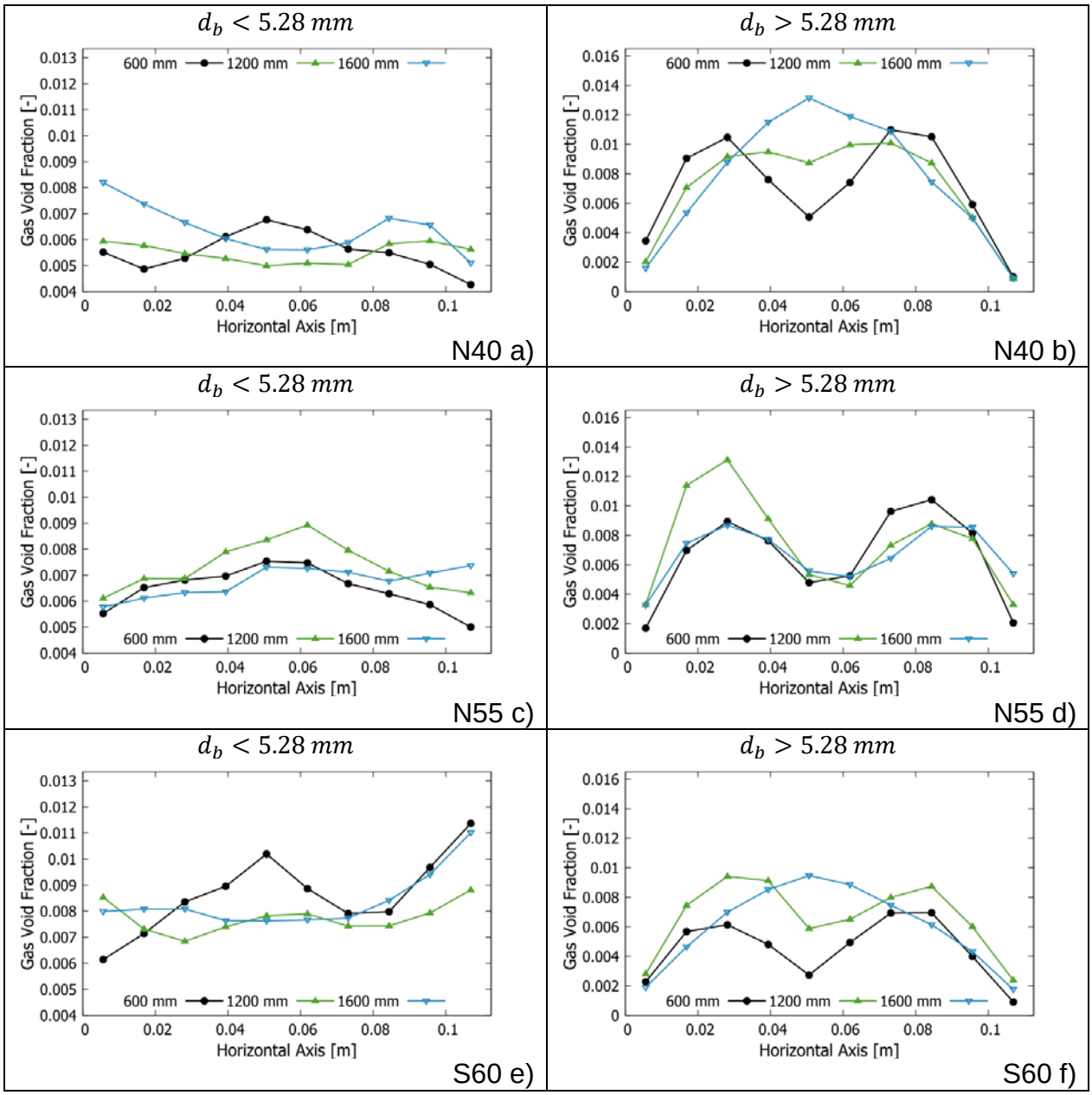

Figure 13 Development of the gas void fraction for bubbles smaller than the critical diameter of 5.28 mm (left column) and larger than the diameter (right column) for case N40 (inhomogeneous), N55 (transition) and S60 (homogenous).

The effects of coalescence are also reflected in Figure 14, which shows the Sauter mean diameters over height. The results show that the stability criterion of Lucas et al. (2), eq. (2) can experimentally confirmed. As a simplified criterion also the gas volume

fraction transported by bubbles larger or smaller than the critical diameter at which the lift force changes its sign can be used, i.e. only two bubble classes are considered for eq. (2). If the fraction of gas transported by small bubbles is larger than the one transported by large bubbles the flow is stabilized and should lead to homogeneous flow regime. Vice versa a larger amount of gas transported by large bubbles leads to a heterogeneous regime. In the transition region both parts are about the same.

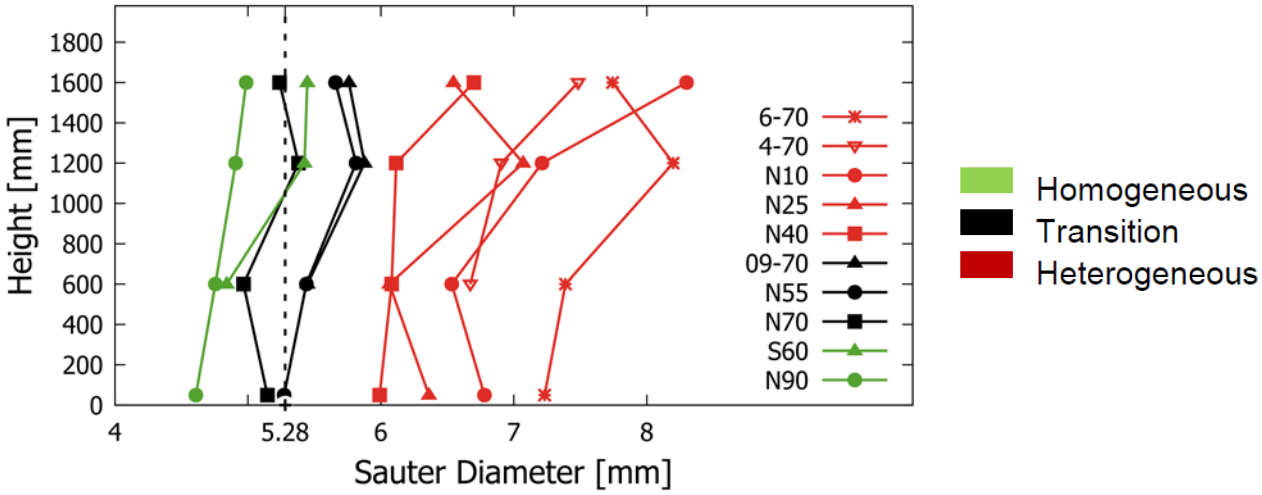

Figure 14 Sauter mean diameters for all experiments and height positions.

The stability criterion was obtained for a spatial homogeneous flow and reflects for this reason the local stability. As discussed by Lucas et al. (2007) for real bubble columns there is always an interaction between local and global stability. Figure 15 shows profiles of the stability parameter for some of the cases discussed above. Again for cases 6-70 and N90 the parameter is clearly negative or positive over all the column width. For cases N70 and S60 the profiles have positive and negative regions which means that parts of the flow are stabilized others destabilized. Since the negative regions are located in the center of the column is can be assumed that the transition from homogeneous to heterogeneous flow starts in the column center. Such local instabilities enhance coalescence and with that the further transition to a global instability and a heterogeneous regime in case the column is long enough.

Inhomogeneous case 6-70

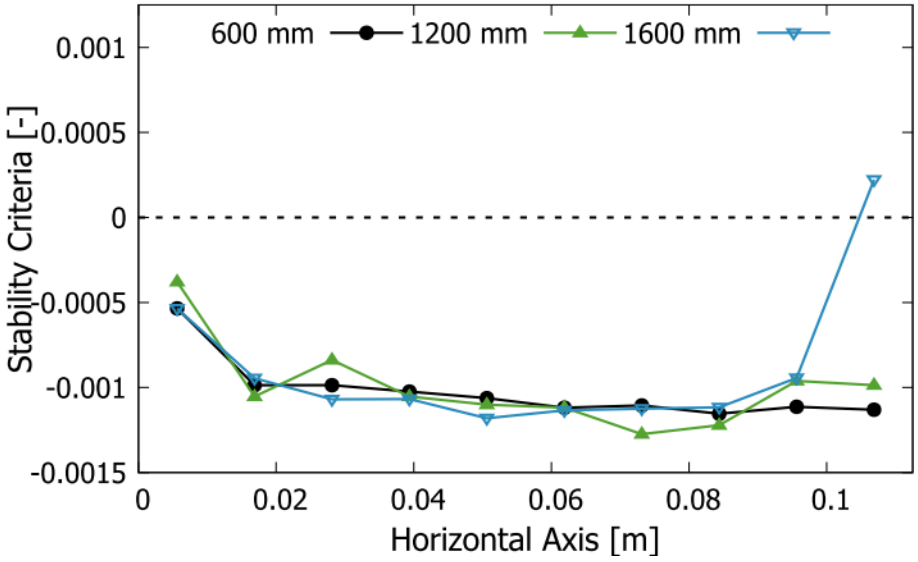

Homogenous case N90

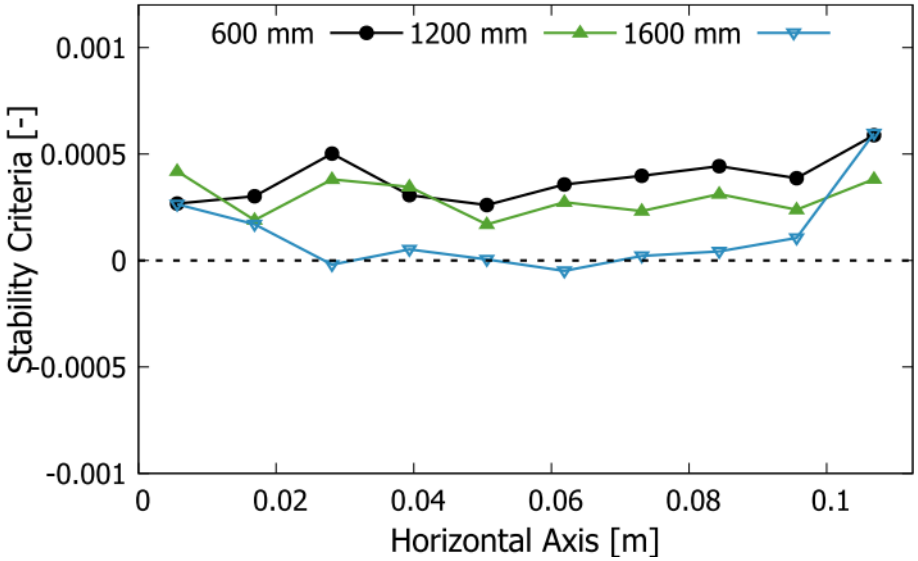

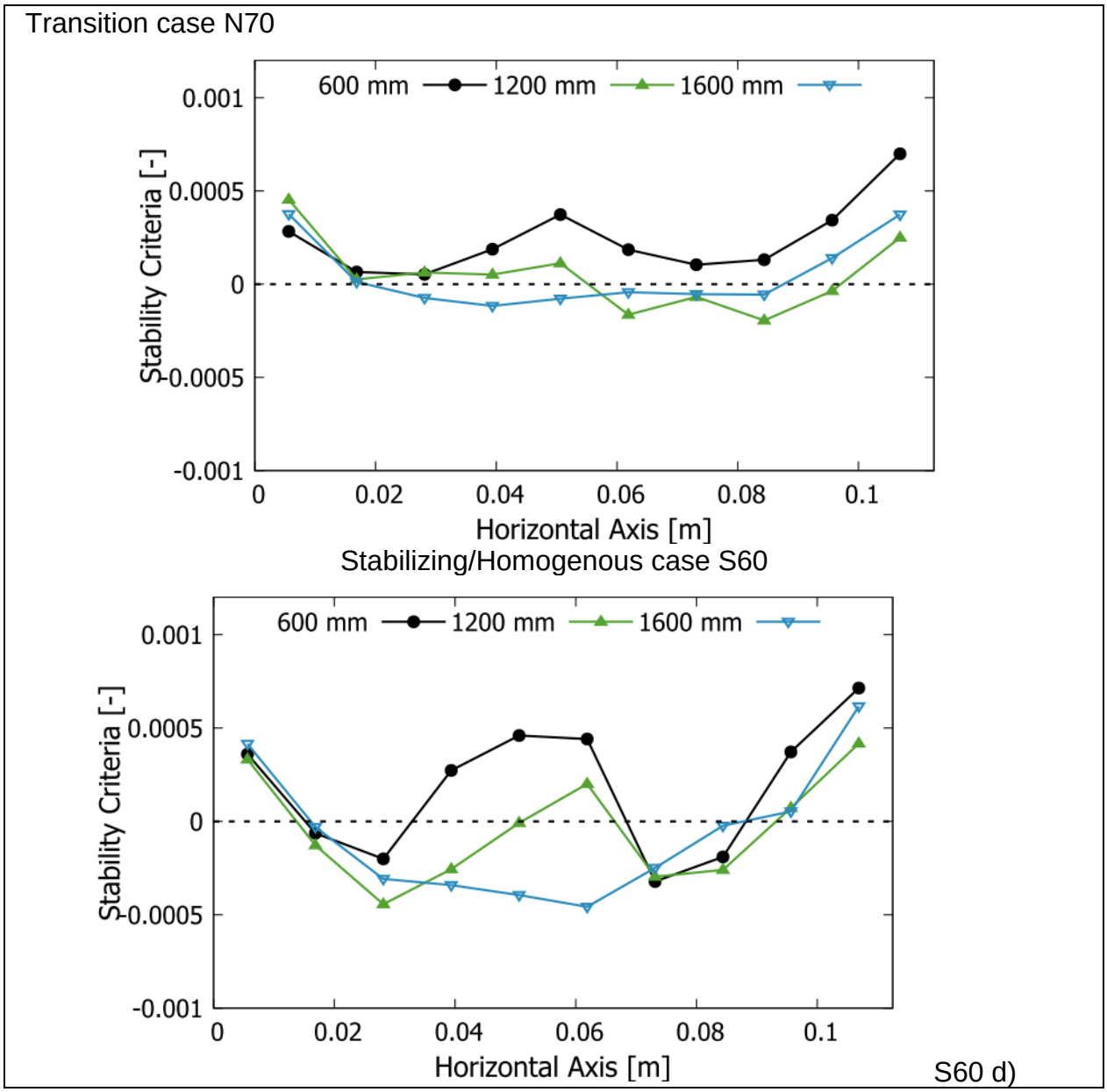

Figure 15 Profiles of the stability criteria for different cases

The locally stable and instable regions are reflected beside the stability parameter in a good approximation also by the averaged bubble size. Figure 16 shows the profile of the Sauter mean diameter for case S60. It can be well seen that the Sauter mean diameter exceeds the critical diameter at which the lift force changes it sign locally. Again there are stabilized and destabilized regions with the destabilizing zone in the column center at the height position of 1600 mm.

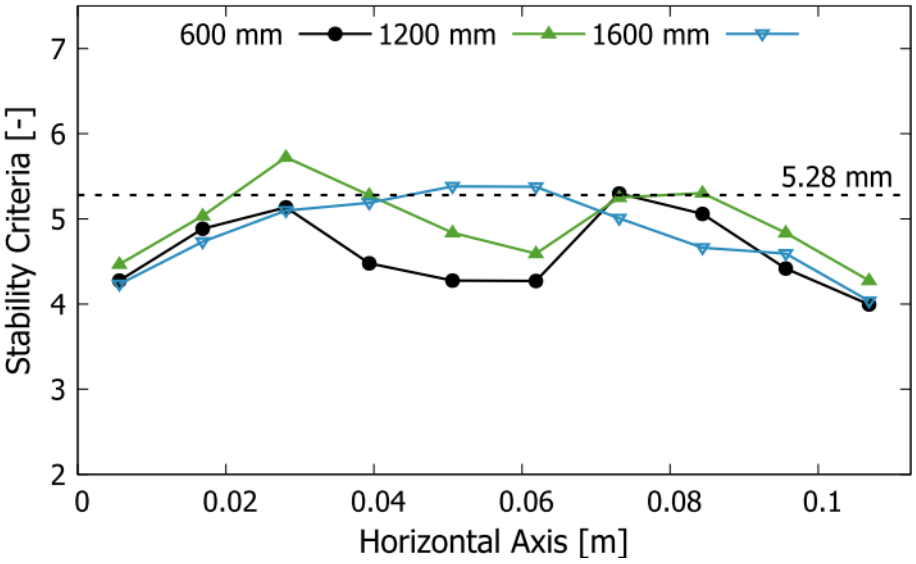

Figure 16 Profile of the Sauter mean diameter for case S60 (homogenous) with the critical lift force diameter of 5.28 mm.

4. Conclusions

The experiments confirm the validity of the stability criterion obtained by Lucas et al. (2005) for poly-disperse bubbly flows. It is shown that the regime transition is triggered by the bubble size distribution. Completely different flow situations are obtained by only changing the bubble size distribution at an unchanged gas flow rate. In case of a positive stability parameter the flow is stabilized and tends to the homogeneous flow regime. A negative parameter in contrast destabilizes the flow leading to a heterogeneous flow regime. This can be explained by the inversion of the lateral lift force in dependence of the bubble size. As a simplification also the fraction of gas volume transported by bubbles smaller and larger than the critical diameter at which the lift force changes its sign can be used. If the larger part is transported by small bubbles the flow is stabilized, otherwise it is destabilized.

It has to be considered that the stability criterion is valid at local scale only. For large scale industrial bubble columns there is always an interaction between local and global stability effects. Also, regarding the lift force in complex systems there are still some open questions as the influence of swarm effects and turbulence. There is also additional complexity for contaminated systems. This may lead to some shift of the critical parameters in industrial applications compared to the ones discussed here. Nevertheless, the critical diameter in low void fraction bubbly flows is almost identical to the value obtained from single bubble experiments as shown in our previous study (Ziegenhein et al., 2019). The investigations clearly show the triggering effect of the lift

force for the transition from the homogeneous to the heterogeneous flow regime in bubble columns. Applying appropriate correlations for drag and lift force together with the information on the bubble size distribution the stability criterion can be used to predict the flow regime.

References

Akbar, M. H. b. M., K. Hayashi, D. Lucas und A. Tomiyama, 2013. Effects of inlet condition on flow structure of bubbly flow in a rectangular column. Chemical Engineering Science 104, 166–176.

Camarasa, E., Vial, C., Poncin, S., Wild, G., Midoux, N., Bouillard, J., 1999. Influence of coalescence behaviour of the liquid and of gas sparging on hydrodynamics and bubble characteristics in a bubble. Chemical Engineering and Processing 38, 329–344.

Dijkhuizen, W., Roghair, I., Van Sint Annaland, M., Kuipers, J. A., 2010. DNS of gas bubbles behaviour using an improved 3D front tracking. Chem. Eng. Sci, 65, 1415–1426.

Harteveld, W., (2005). Bubble columns, Structures or stability? Ph.D. Thesis, Technische Universiteit Delft, ISBN: 90-64642-26-5.

Hessenkemper, H. & Ziegenhein, T., 2018. Particle Shadow Velocimetry (PSV) in bubbly flows. International Journal of Multiphase Flow 106, 268-279

Kazakis, N. A., Papadopoulos, I. D., Mouza, A. A., (2007). Bubble columns with fine pore sparger operating in the pseudo-homogeneous regime: Gas hold up prediction and a criterion for the transition to the heterogeneous regime. Chemical Engineering Science 62, 3092–3103.

Krishna, R., Wilkinson, P. M., van Dierendonck, L. L., 1991. A Model for Gas Holdup in bubble-Columns Incorporating the Influence of Gas Density on Flow Regime ransitions. Chemical Engineering Science 46, 2491–2496.

León-Becerril, E., Liné, A., 2001. Stability of a bubble column. Chemical Engineering Science 56, 6135–6141.

Lucas, D., Prasser, H.-M., Manera, A., 2005. Influence of the lift force on the stability of a bubble column, Chem. Eng. Sci, 60, 3609-3619.

Lucas, D., Prasser, H.-M., Manera, A. , 2007. Stability effect of the lateral lift force in bubbly flows, International Conference on Multiphase Flow, Leipzig, Germany.

Mudde, R. F., Harteveld, W. K., van den Akker, H. E. A., (2009). Uniform Flow in bubble-Columns. Ind. Eng. Chem. Res. 48, 148–158.

Reilly, I. G., Scott, D. S., de Bruijn, T. J. W., MacIntyre, D., 1994. The Role of Gas Phase Momentum in Determining Gas Holdup and Hydrodynamic Flow Regimes in Bubble Column Operations. The Canadian Journal of Chemical Engineering 72, 3–12.

Ribeiro, C. P. (2008). On the estimation of the regime transition point in bubble columns. Chemical Engineering Journal 140, 473–482.

Ruzicka, M., Zaradník, J., Drahoš, J., Thomas, N. 2001. “Homogeneous–heterogeneousregime transition in bubble columns. Chemical Engineering Science 56, 4609–4626.

Ruzicka, M., Drahos, J., Mena, P., Teixeira, J., 2003. Effect of viscosity on homogeneous and heterogeneous flow regime transition in bubble columns. Chemical Engineering Journal 96, 15–22.

Ruzicka, M.C., Vecer, M.M. Orvalho, S. Drahoš, J., 2008. Effect of surfactant on homogeneous regime stability in bubble column. Chemical Engineering Science 63, 951 – 967.

Sarrafi, A., Jamialahmadi, M., Mueller-Steinhagen, H., Smith, J. M., 1999. Gas Holdup in Homogeneous and Heterogeneous Gas-Liquid Bubble Column Reactors. The Canadian Journal of Chemical Engineering 77, 11–21.

Sharaf, S., Zednikova, M., Ruzicka, M.C., Azzopardi, B.J., 2016. Global and local hydrodynamics of bubble columns – Effect of gas distributor. Chem. Eng. J. 288, 489-504.

Tomiyama, A., 1998. Struggle with computational bubble dynamics. IThird International Conference on Multiphase Flow, ICMF’98, Lyon, France.

Tomiyama, A., Tamai, H., Zun, I., Hosokawa, S., 2002. Transverse migration of single bubbles in simple shear flows, Chem. Eng. Sci,. 57, 1849–1858.

Wellek, R. M., Agrawal, A. K., Skelland, A. H. P., 1966. Shape of Liquid Drops Moving in Liquid Media. AlChE Journal 12, 854.

Wilkinson, P. M., Spek, A. P., van Dierendonck, L. L., 1992. Design Parameters Estimation for Scale-Up of High-pressure Bubble Columns. AIChE Journal 38.544-554.

Xu S., Qu, Y., Chaouki, J., Guy, Ch., 2005. Characterization of homogeneity of bubbe flows in buble columns using RPT and fibre optics. International Journal of Chemical Reactor Engineering, 3, A54.

Zahradnik, J., Fialova, M., Ruzicka, M., Drahos, J., Kastanek, F., N. Thomas, N., 1997. Duality of the gas-liquid flow regimes in bubble column reactors. Chemical Engineering Science 52, 3811.

Ziegenhein, T. & Lucas, D., 2016. On sampling bias in multiphase flows: Particle image velocimetry in bubbly flow. Flow Measurement and Instrumentation 48, 36–41.

Ziegenhein, T., Zalucky, J., Rzehak, R., Lucas, D., 2016. On the hydrodynamics of airlift reactors, Part I: Experiments. Chem. Eng. Sci,. 150, 54–65.

Ziegenhein, T. & Lucas, D., 2017. Observations on bubble shapes in bubble columns under different flow conditions, Experimental Thermal and Fluid Science 85, 248-256.

Ziegenhein, T., Tomiyama, A., Lucas, D., 2018. A new measuring concept to determine the lift force for distorted bubbles in low Morton number system: Results for air/water. International Journal of Multiphase Flow 108, 11-24.

Ziegenhein, T. & Lucas, D., 2019. The critical bubble diameter of the lift force in technical and environmental, buoyancy-driven bubbly flows. International Journal of Multiphase Flow, submitted.

Zun, I. (1980). The transverse migration of bubbles influenced by walls in vertical bubbly flow. International Journal of Multiphase Flow, 6, 583-588.